

**ILJS-24-053 (SPECIAL EDITION)****Enhancing Efficiency and Performance of Non-Fullerene Acceptor-Based Organic Solar Cells with Graphene Interlayer via Numerical Simulation****Muhammed O. A.^{1,3}, Sebastian W.¹, Geoffrey O. B.², Julius M. M.¹**¹Department of Physics, University of Nairobi, P. O. Box 30197-00100 Nairobi, Kenya.²Department of Chemistry, University of Nairobi, P. O. Box 30197-00100 Nairobi, Kenya.³Department of Physics, Confluence University of Science and Technology, Osara, Kogi State, Nigeria.**Abstract**

Non-fullerene acceptor (NFA) based organic solar cells (OSCs) have the potential to be low-cost and highly efficient next-generation solar cells via interfacial engineering. Herein, we adopt a computational approach to analyse the effect of surface passivation material (graphene) in reducing interfacial recombination while also promoting the extraction of holes in an OSC architecture with the absorbing layer comprising a donor polymer poly[4,8-bis(5-(2-ethylhexyl)thiophen-2-yl)benzo[1,2-b;4,5-b']dithiophene-2,6-diyl-alt-(4-(2-ethylhexyl)-3-fluorothieno[3,4-b]thiophene)-2-carboxylate-2,6-diyl] (PTB7-Th) and an NFA 3,9-bis(2-methylene-(3-(1,1-dicyanomethylene)-indanone))-5,5,11,11-tetrakis(5-hexylthienyl)-dithieno[2,3-d:2',3'-d']-s-indaceno [1,2-b:5,6-b']dithiophene (ITIC-Th). SCAPS-1D software was used to model the impact of the graphene layer in the NFA-OSC by analysing the thicknesses of the graphene, absorbing layer, and hole transport layer (HTL), coupled with the analysis of the doping concentration of the HTL, the defect density of the absorbing layer, the interfacial defect densities at the absorbing layer/graphene and the graphene/HTL with the device structure: ITO/ZnO/PTB7-Th: ITIC-Th/Graphene/PEDOT: PSS/Au. A power conversion efficiency (PCE) of 6.2163% was obtained during the initial simulation of the device without graphene, while a PCE of 11.6607% was obtained for the device with graphene, showing a low recombination effect in the device. Upon carefully optimising the design of the device with graphene, an efficiency of 20.1967% was obtained, a 73% increase in efficiency over the initial design. This study demonstrates that the addition of adding graphene as a layer, helps to mitigate loss in energy and improves electric charge flow, making this solar cell efficient.

Keyword: non-fullerene acceptors; organic solar cells; graphene; interfacial defect; doping concentration.**1. Introduction**

Thin film-based organic photovoltaics (OPVs) have emerged as one of the major competitors in the photovoltaic research industry, due to advantages such as easy synthetic route, flexibility, semi-transparent nature, low environmental impact, rapid energy payback (Haris et al., 2024), highly adjustable photo-absorption, and lightweight properties (Wang et al., 2024). The absorbing or active layer of OPVs comprises bulk-heterojunction (BHJ) film of donor-acceptor (D-A) organic semiconducting compounds, for D, is a p-type electron donor while A is an n-type electron acceptor (Yu et al., 1995; Heeger, 2013).

In recent years, the emergence of non-fullerene acceptors (NFAs) having intrinsic properties like

Corresponding Author: Muhammed O. A.

Email: abdulmalikmo@students.uonbi.ac.ke

tunable optical absorption, planar architecture, matching band energy level (Wei et al., 2020; Zhao et al., 2017; Yuan et al., 2019; Zhu et al., 2021; Cheng et al., 2018; Ma et al., 2020), and broad photo-absorption range close to the near infra-red (NIR) regions of the EM spectrum (Chen et al., 2014) contributed to the rapid development of OPVs.

The hole transport layer (HTL) is crucial in determining the photovoltaic performance of OPVs. Poly (3, 4-ethylene dioxythiophene) polystyrene sulfonate (PEDOT: PSS) is a widely utilised HTL for OPVs (Nithya & Sudheer, 2020). The reliability and suitability of this semiconducting material as HTL in OPVs is due to its electrical conductivity value of up to 1000 S cm^{-1} , optically transparent in the visible range of the EM spectrum with a value greater than 90%, and its high work function of 5 eV (Mehrabian et al., 2021). Nonetheless, the hygroscopic and acidic nature of PEDOT: PSS is responsible for degrading optoelectronic devices (Nithya & Sudheer, 2020).

Graphene is employed in photovoltaics due to its exceptional properties such as excellent charge mobility capabilities, great stability, resistance to moisture and high optical transmittance (Danladi et al., 2023). An efficient carrier charge extraction, transport and collection can be enhanced at the active layer-HTL interface, leading to an improved electrical contact when graphene is used as an interfacial layer (Muchuweni et al., 2020).

Despite the advancements of in efficiency enhancements in OSCs, charge transport and stability of these devices still remains an issue. PTB7-Th: ITIC-Th photo-active layer have shown promising efficiency; however, efficient charge extraction and long-term stability need improvement. Interfacial modification between photo-active and charge transport layers have shown to enhance device performance and reduce recombination losses. The introduction of graphene herein as an interfacial layer between the photo-active and hole transport layer has the potential to improve stability and charge selectivity as well as optimizing the performance of PTB7-Th: ITIC-Th based OSCs. Hence, this work aims to explore graphene integration into the OSCs structure via a simulation technique and parametric optimization in order to address the inherent challenges of OSCs, improving charge carriers transport and enhancing the overall efficiency of the photovoltaic device.

The integration of graphene has been utilised in solar cells, however its specific role and interaction as being sandwiched in this donor-acceptor interface layer have not been thoroughly investigated. This provides potentially new strategy in OSCs stability and charge transport enhancements and advance its practical application towards interfacial modification.

2. Materials and Methods

2.1 Modelling and Simulation Methodology

2.1.1 Methodology

This study aims to investigate the impact of graphene as an interfacial layer between the active layer and HTL of the solar cell device by optoelectronic simulation technique using SCAPS-1D version 3.3.10, a software suitable for simulating similar photovoltaic devices (Burgelman et al., 2013). Utilising three fundamental semiconductor equations that regulate charge carrier behaviour in photovoltaic devices, the software numerically models the PV parameters of the OPV device. These equations are Poisson's equation (equation 1), the carrier continuity equation (equations 2 & 3), and the drift-diffusion equation (equations 4 & 5).

$$\frac{d^2\phi(x)}{dx^2} = \frac{q}{\epsilon_0\epsilon_r} (p(x) - n(x) + N_D^+ - N_A^- + p_{trap}(x) - n_{trap}(x)) \quad (1)$$

$$-\frac{1}{q} \frac{dJ_n}{dx} = R_n(x) - G(x) \quad (2)$$

$$\frac{1}{q} \frac{dJ_p}{dx} = R_p(x) - G(x) \quad (3)$$

$$J_n = qn(x)\mu_n \frac{d\phi(x)}{dx} + qD_n \frac{dn(x)}{dx} \quad (4)$$

$$J_p = qp(x)\mu_p \frac{d\phi(x)}{dx} + qD_p \frac{dp(x)}{dx} \quad (5)$$

where ϕ is electrical potential, ϵ_0 is the absolute dielectric constant, ϵ_r is the relative dielectric constant of each material layer, q is the electric charge, N_A^-/N_D^+ are the acceptor/donor doping density, n_{trap}/p_{trap} are the trap density for electrons/holes, and $n(x)/p(x)$ are the electron/hole density as a function of the thickness, x , J_n/J_p are the electron/hole current density, G is the carrier photogeneration, and R_p/R_n are carrier recombination rates of holes/electrons respectively. μ_p/μ_n are the mobility of hole/electron, D_p/D_n are the hole/electron diffusion coefficient.

2.1.2 Simulation Parameters and Structure of the Device

The device is an inverted organic solar cell structure with the transparent conducting oxide as Indium Tin Oxide (*ITO*), ETL as Zinc Oxide (*ZnO*), active layer as *PTB7-Th: ITIC-Th*, the passivation layer as graphene, HTL as *PEDOT: PSS*, and the back-contact electrode as gold (*Au*) This study utilises the conventional illumination solar spectrum (AM 1.5G) and a scanning voltage of 0 - 1.5 V at an operating temperature of 300 K. The structure of the device is shown in Fig. 1.

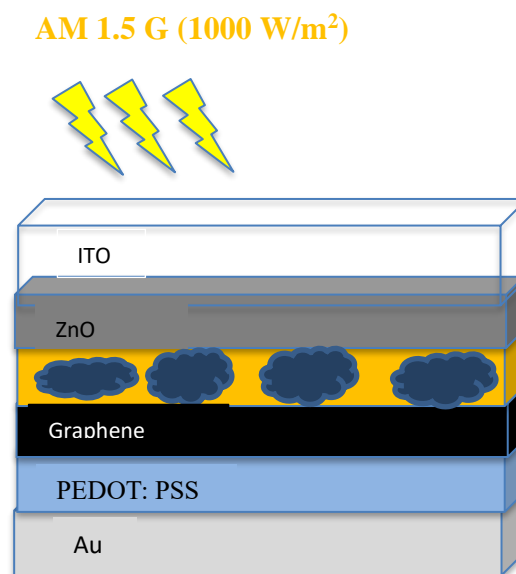


Figure 1. Configuration of the organic solar cell device.

3. Result and Discussion

3.1 Initial device with and without graphene

The role of graphene as an interfacial between the active layer and the HTL improves the photovoltaic parameters of the device as shown in Fig. 2, resulting in improvements with 88% in PCE, 83% in short-circuit current density (J_{sc}), and 2.7% in open-circuit voltage (V_{oc}) when compared to the initial device without graphene. These improvements are attributed to enhanced charge carrier transfers at the active layer/graphene interface and the suppression of non-radiative recombination losses (Danladi et al., 2023).

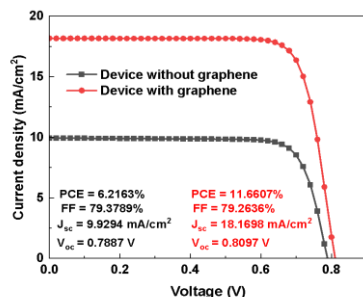


Figure 2. The current density-voltage curve of initial devices with and without graphene.

3.2 Influence of Graphene thickness

The variation in the current density-voltage (J-V) curve with the thickness of the graphene layer ranging from 0.3 to 1.3 μm is depicted in Fig. 3a, while Fig. 3b depicts the PV performance metrics of the device. As the thickness of graphene increases, all the PV parameters increase except for FF, the increment of PCE, J_{sc} , and V_{oc} could be attributed to a higher rate of photon absorption and a better charge carrier collection at the interface, while high lateral resistance is induced at the interface, leading to a decrease in FF (Kang et al., 2019). The thickness value of 1.3 μm was chosen as the optimum.

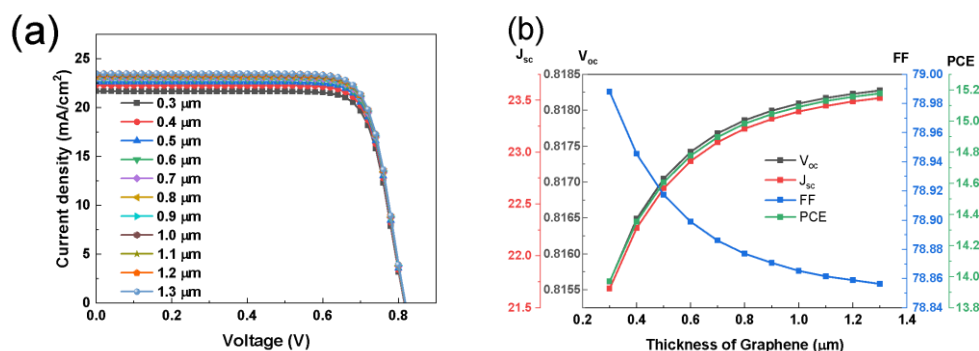


Figure 3. (a) Variation in J-V curve with thickness of graphene under illumination (b) Variation in J_{sc} , V_{oc} , FF, and PCE with the thickness of graphene.

3.3 Influence of HTL thickness on the device with graphene

When suitable HTLs are selected for OPV devices, enhanced charge carrier transport and collection are observed. The J-V characteristics of the device as the thickness of the HTL increases from 0.02 – 0.11 μm are shown in Fig. 4a, while the PV parameters are shown in Fig. 4b. The PCE, J_{sc} , and V_{oc} increases steadily as the thickness of the HTL increases, this shows that majority of charge carrier separation occurs in the active layer (Nithya & Sudheer, 2020). The decrease in FF is due to the increases in series resistance of the device as HTL thickness increases. An optimum thickness value of 0.11 μm was chosen for the HTL.

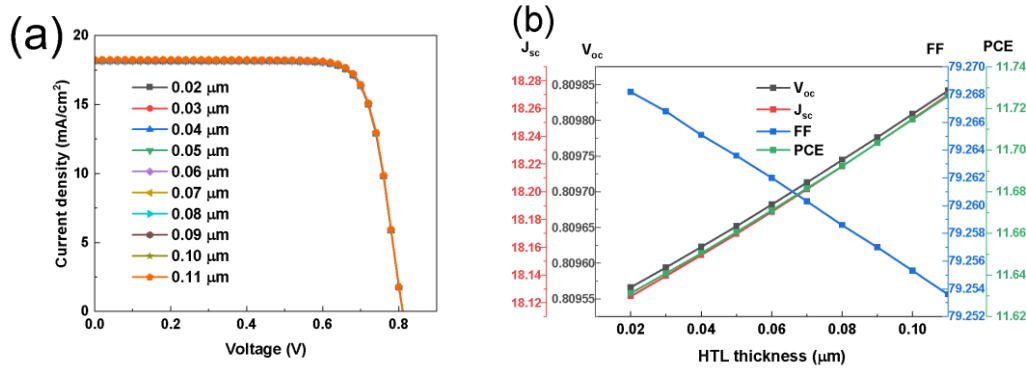


Figure 4. (a) Variation in J-V curve with HTL thickness under illumination (b) Variation in J_{sc} , V_{oc} , FF, and PCE with HTL thickness.

3.4 Influence of Absorbing layer thickness on the device with graphene

The thickness of the active layer is varied from 0.1 – 1.0 μm, and the corresponding J-V behaviour and variation in PV parameters are depicted in Fig. 5a and 5b respectively. The PCE, J_{sc} , and V_{oc} increase to a thickness value of 0.3 μm, indicating an optimum thickness for the device, due to improved photo absorption and more generation of charge carriers. However, the FF continuously declines as the thickness of the active layer increases due to an increment of series resistance in the device (Abdelaziz et al., 2019).

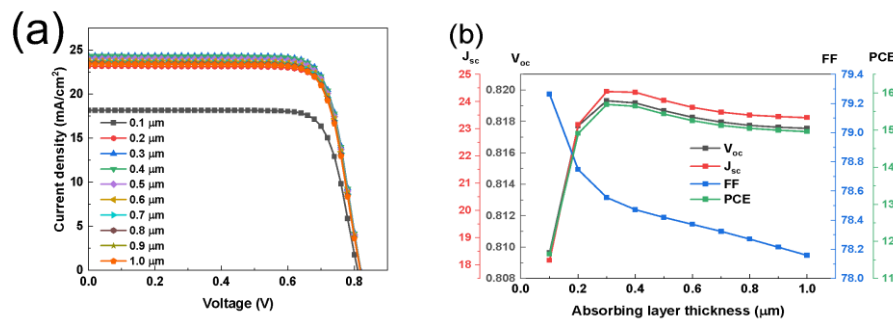


Figure 5. (a) Variation in J-V curve with absorbing layer thickness under illumination (b) Variation in J_{sc} , V_{oc} , FF, and PCE with absorbing layer thickness.

3.5 Influence of Absorbing layer defect density on the device with graphene

The active layer of PV devices generates photoelectrons upon photon absorption, an increase in defect density (N_t) of this layer occurs if the quality of the thin film is poor, thereby affecting the V_{oc} (Muhammed et al., 2021). The impact of the defect density on this layer is analysed using the Shockley-Read-Hall (SRH) recombination model (Wolff et al., 2019). The defect density of the absorbing layer was varied from 10^{10} to 10^{16} cm⁻³, with Fig. 6a and 6b showing the J-V curve and the relationship between the PV parameters with an increasing N_t . The PV output performance deteriorates as the N_t of the absorbing layer increases due to the increase in carrier recombination (Abdulmalik et al., 2022). The optimum value for defect density for the absorbing layer was chosen as 10^{10} cm⁻³.

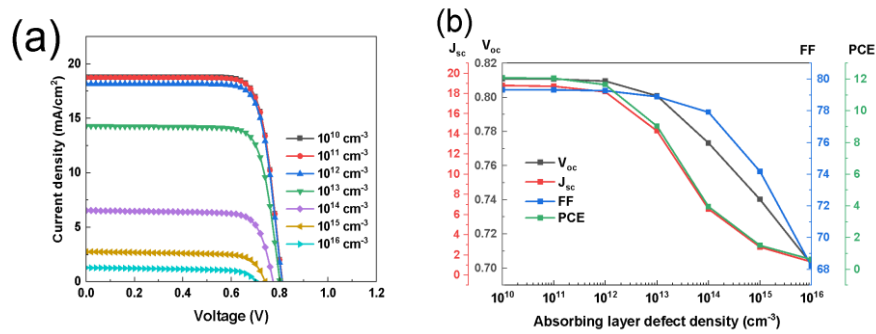


Figure 6. (a) Variation in J-V curve with absorbing layer defect density under illumination (b) Variation in J_{sc} , V_{oc} , FF, and PCE with absorbing layer defect density.

3.6 Influence of interface defect density (Absorbing layer/graphene) on the device with graphene

The impact of an increased defect density at the absorbing layer/graphene interface on the device performance is shown in Fig. 7a and 7b. The interfacial trap densities can increase either from ion drift or device degradation (Kang et al., 2019). The interface defect density was varied from 10^5 to 10^{12} cm⁻² and Fig. 7a and 7b show the J-V curves and PV parameters respectively. Increasing the interface defect density shows a degradation in PCE, J_{sc} , and V_{oc} which could be due to the limited charge carrier collection at the interface, and a possible means of charge carrier transport leading to an increment in FF. The chosen optimum interface defect density value was 10^{05} cm⁻².

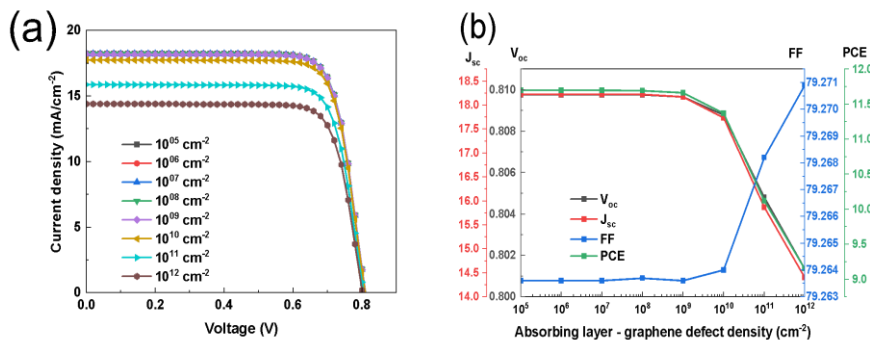


Figure 7. (a) Variation in J-V curve with absorbing layer – graphene interface defect density under illumination (b) Variation in J_{sc} , V_{oc} , FF, and PCE with absorbing layer - graphene interface defect density.

3.7 Influence of Graphene/HTL interface defect density on the device with graphene

The discontinuity between two layers at the interfaces in the architecture of PV devices often leads to the induction of localised defect states (Rahman et al., 2019). The interface defect density between graphene and the HTL was investigated by varying the defect density from 10^6 to 10^{13} cm⁻². Fig. 8a shows the J-V curve with this variation, while Fig. 8b shows the relationship between J_{sc} , V_{oc} , FF, and PCE to the defect densities. As the interface defect density increases, a downward trend was noticeable in J_{sc} , V_{oc} , and PCE, and an unusual trend was observed in the FF which could be the result of improved charge extraction created by higher interfacial defects. The optimum interface defect density was chosen as 10^{06} cm⁻².

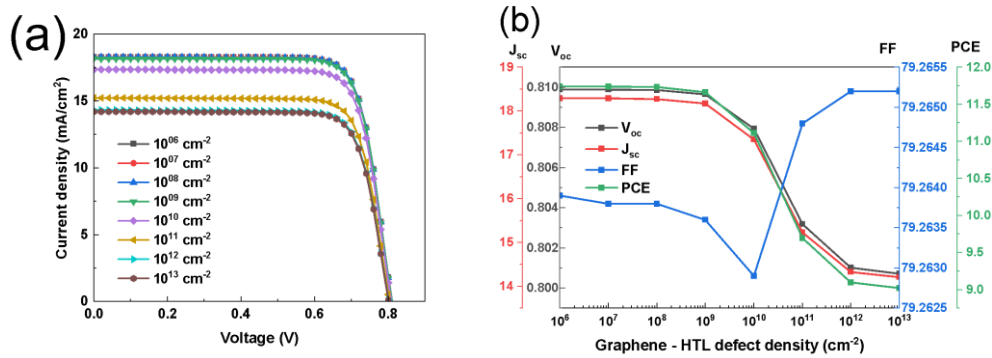


Figure 8. (a)Variation in J-V curve with graphene-HTL interface defect density under illumination (b) Variation in J_{sc} , V_{oc} , FF, and PCE with graphene-HTL interface defect density.

3.8 Influence of HTL doping concentration on the device with graphene

An increment of the doping concentration of the HTL leads to an increased device conductivity while reducing series resistance in the device (Nithya & Sudheer, 2020). The doping concentration of the HTL was varied from 10¹³ to 10²⁰ cm⁻³. Fig. 9a shows the J-V curves with the doping concentration, while Fig. 9b depicts the response of the PV parameters with this range. The FF increases as the doping concentration of the HTL increases to a limit which cannot exceed, as seen in Fig. 9b, a result of the saturation of the HTL’s sheet resistance and conductivity. The optimum value of HTL doping concentration was taken as 10²⁰ cm⁻³.

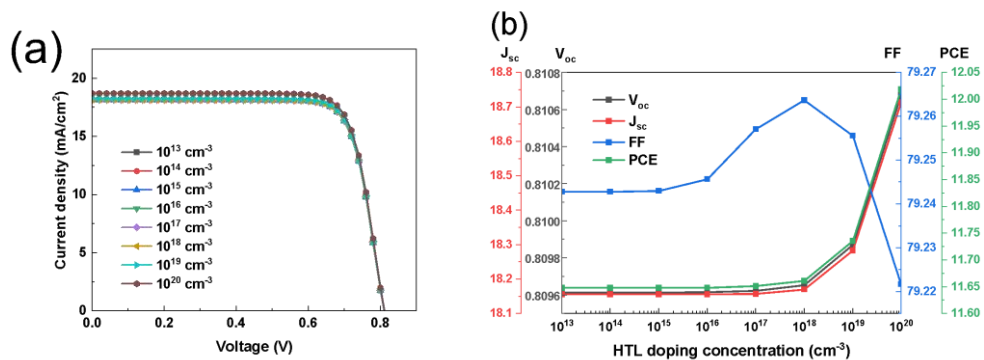


Figure 9. (a)Variation in J-V curve with HTL doping concentration under illumination (b) Variation in J_{sc} , V_{oc} , FF, and PCE with HTL doping concentration.

3.9 Performance of optimised device

The optimised OPV device simulated shows enhanced PV parameters when compared to the initial device without a graphene layer and the unoptimised device with a graphene layer as shown in Fig. 10. The results from the optimisation of the device with graphene are PCE of 20.1967%, FF of 78.3125%, J_{sc} of 31.1383 mA/cm², and V_{oc} of 0.8282 V. A 73% increase in PCE, a 71% increase in J_{sc} , and a 2.5% increase in V_{oc} are observed when the optimised device with graphene was compared with the unoptimised device with graphene.

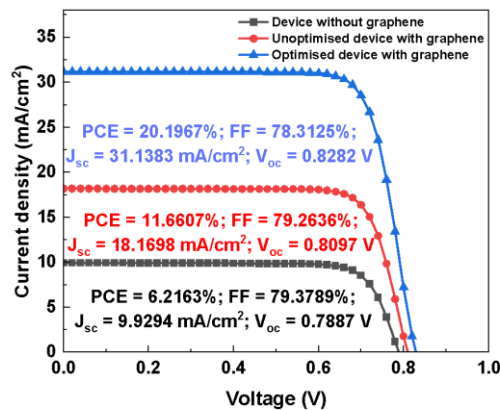


Figure 10. J–V curves of the device without graphene (black), unoptimised device with graphene (red) and optimised device with graphene (blue).

4. Conclusion

In this study of a non-fullerene acceptor-based organic solar cell, in which graphene was employed as an interfacial between the active and the HT layers, the SCAP-1D simulation software was used to investigate how the graphene layer affects the photovoltaic parameters of the device. The device without graphene was initially simulated, with the following PV parameters obtained; PCE of 6.2163%, FF of 79.3789%, J_{sc} of 9.9294 mA/cm², and V_{oc} of 0.7887 V. The device was modified by incorporating graphene leading to the device structure: *ITO/ZnO/PTB7-Th: ITIC-Th/graphene/PEDOT: PSS/Au*, for this unoptimised structure, the PV parameters obtained from the simulation were a PCE of 11.6607%, FF of 79.2636%, J_{sc} of 18.1698 mA/cm², and V_{oc} of 0.8097 V. The effects of the thickness of graphene, the thickness of HTL, the thickness of the active layer, the defect density of the active layer, the active layer/graphene, graphene/HTL interface defect densities, and the doping concentration of the HTL were examined for the graphene incorporated device. The performance metrics of these optimised parameters were; PCE of 20.1967%, FF of 78.3125%, J_{sc} of 31.1383 mA/cm², and V_{oc} of 0.8282 V. These findings indicate the effect of graphene as an interfacial layer between the active and hole transport layer of NFA based organic solar cells owing to proper parameter optimisation technique when employed experimentally for OPV devices.

Acknowledgement

The authors would like to thank Professor Marc Burgelman and his team from the Department of Electronics and Information Systems, University of Ghent, Belgium, for the development of the SCAPS software package and for allowing its use. The authors also wish to extend their gratitude to the University of Nairobi, Kenya and PASET-Regional Scholarship and Innovation Fund (RSIF) for their support and financial contributions to this research endeavour.

References

- Abdelaziz, W., Shaker, A., Abouelatta, M., & Zekry, A. (2019). Possible efficiency boosting of non-fullerene acceptor solar cell using device simulation. *Optical Materials*, *91*, 239–245. <https://doi.org/10.1016/j.optmat.2019.03.023>
- Abdulmalik, M. O., Danladi, E., Obasi, R. C., Gyuk, P. M., Salifu, F. U., Magaji, S., Egbugha, A. C., & Thomas, D. (2022). Numerical study of 25.459% alloyed inorganic Lead-Free Perovskite CSSNGEi3-Based solar cell by device simulation. *East European Journal of Physics*, *4*, 125–135. <https://doi.org/10.26565/2312-4334-2022-4-12>

- Burgelman, M., Decock, K., Khelifi, S., & Abass, A. (2013). Advanced electrical simulation of thin film solar cells. *Thin Solid Films*, 535, 296–301. <https://doi.org/10.1016/j.tsf.2012.10.032>
- Chen, C., Chang, W., Yoshimura, K., Ohya, K., You, J., Gao, J., Hong, Z., & Yang, Y. (2014). An efficient Triple-Junction polymer solar cell having a power conversion efficiency exceeding 11%. *Advanced Materials*, 26(32), 5670–5677. <https://doi.org/10.1002/adma.201402072>
- Cheng, P., Li, G., Zhan, X., & Yang, Y. (2018). Next-generation organic photovoltaics based on non-fullerene acceptors. *Nature Photonics*, 12(3), 131–142. <https://doi.org/10.1038/s41566-018-0104-9>
- Danladi, E., Egbugha, A. C., Obasi, R. C., Tasie, N. N., Achem, C. U., Haruna, I. S., & Ezeh, L. O. (2023). Defect and doping concentration study with series and shunt resistance influence on graphene-modified perovskite solar cell: A numerical investigation in SCAPS-1D framework. *Journal of the Indian Chemical Society*, 100(5), 101001. <https://doi.org/10.1016/j.jics.2023.101001>
- Haris, M., Ryu, D. H., Ullah, Z., Kang, B. J., Jeon, N. J., Lee, S., Lee, H. K., Lee, S. K., Lee, J., Kwon, H., Shin, W. S., & Song, C. E. (2024). Morphological modulation enabled by non-halogenated solvent-processed simple solid additives for high-efficiency organic solar cells. *EcoMat*, 6(3). <https://doi.org/10.1002/eom2.12436>
- Heeger, A. J. (2013). 25th Anniversary article: Bulk Heterojunction Solar Cells: Understanding the Mechanism of Operation. *Advanced Materials*, 26(1), 10–28. <https://doi.org/10.1002/adma.201304373>
- Kang, A. K., Zandi, M. H., & Gorji, N. E. (2019). Simulation analysis of graphene contacted perovskite solar cells using SCAPS-1D. *Optical and Quantum Electronics*, 51(4). <https://doi.org/10.1007/s11082-019-1802-3>
- Ma, R., Liu, T., Luo, Z., Guo, Q., Xiao, Y., Chen, Y., Li, X., Luo, S., Lu, X., Zhang, M., Li, Y., & Yan, H. (2020). Improving open-circuit voltage by a chlorinated polymer donor endows binary organic solar cells efficiencies over 17%. *Science China. Chemistry*, 63(3), 325–330. <https://doi.org/10.1007/s11426-019-9669-3>
- Mehrabian, M., Afshar, E. N., & Yousefzadeh, S. A. (2021). Simulating the thickness effect of the graphene oxide layer in CsPbBr₃- based solar cells. *Materials Research Express*, 8(3), 035509. <https://doi.org/10.1088/2053-1591/abf080>
- Muchuweni, E., Martincigh, B. S., & Nyamori, V. O. (2020). Organic solar cells: Current perspectives on graphene-based materials for electrodes, electron acceptors and interfacial layers. *International Journal of Energy Research*, 45(5), 6518–6549. <https://doi.org/10.1002/er.6301>
- Muhammed, O. A., Danladi, E., Boduku, P., Tasiu, J., Ahmad, M., & Usman, N. (2021). Modeling and simulation of Lead-Free Perovskite Solar Cell using SCAPS-1D. *East European Journal of Physics*, 2. <https://doi.org/10.26565/2312-4334-2021-2-12>
- Nithya, K., & Sudheer, K. (2020). Device modelling of non-fullerene organic solar cell with inorganic CuI hole transport layer using SCAPS 1-D. *Optik*, 217, 164790. <https://doi.org/10.1016/j.ijleo.2020.164790>
- Rahman, M. S., Miah, S., Marma, M. S. W., & Sabrina, T. (2019). *Simulation based investigation of inverted planar perovskite solar cell with all metal oxide inorganic transport layers*. <https://doi.org/10.1109/ecace.2019.8679283>
- Wang, J., Wang, C., Wang, Y., Qiao, J., Ren, J., Li, J., Wang, W., Chen, Z., Yu, Y., Hao, X., Zhang, S., & Hou, J. (2024). Pyrrole-Based fully non-fused acceptor for efficient and stable organic solar cells. *Angewandte Chemie*, 63(15). <https://doi.org/10.1002/anie.202400565>
- Wei, Q., Liu, W., Leclerc, M., Yuan, J., Chen, H., & Zou, Y. (2020). A-DA'D-A non-fullerene acceptors for high-performance organic solar cells. *Science China. Chemistry*, 63(10), 1352–1366. <https://doi.org/10.1007/s11426-020-9799-4>
- Wolff, C. M., Caprioglio, P., Stolterfoht, M., & Neher, D. (2019). Nonradiative recombination in perovskite solar cells: the role of interfaces. *Advanced Materials*, 31(52). <https://doi.org/10.1002/adma.201902762>
- Yu, G., Gao, J., Hummelen, J. C., Wudl, F., & Heeger, A. J. (1995). Polymer photovoltaic cells: enhanced efficiencies via a network of internal Donor-Acceptor heterojunctions. *Science*, 270(5243), 1789–1791. <https://doi.org/10.1126/science.270.5243.1789>

- Yuan, J., Zhang, Y., Zhou, L., Zhang, G., Yip, H., Lau, T., Lu, X., Zhu, C., Peng, H., Johnson, P. A., Leclerc, M., Cao, Y., Ulanski, J., Li, Y., & Zou, Y. (2019). Single-Junction Organic Solar Cell with over 15% Efficiency Using Fused-Ring Acceptor with Electron-Deficient Core. *Joule*, 3(4), 1140–1151. <https://doi.org/10.1016/j.joule.2019.01.004>
- Zhao, W., Li, S., Yao, H., Zhang, S., Zhang, Y., Yang, B., & Hou, J. (2017). Molecular Optimization Enables over 13% Efficiency in Organic Solar Cells. *Journal of the American Chemical Society*, 139(21), 7148–7151. <https://doi.org/10.1021/jacs.7b02677>
- Zhu, L., Zhang, M., Zhong, W., Leng, S., Zhou, G., Zou, Y., Su, X., Ding, H., Gu, P., Liu, F., & Zhang, Y. (2021). Progress and prospects of the morphology of non-fullerene acceptor based high-efficiency organic solar cells. *Energy & Environmental Science*. <https://doi.org/10.1039/d1ee01220g>